Optics Letters

Photonic microwave harmonic down-converter based on stabilized period-one nonlinear dynamics of semiconductor lasers

PEI ZHOU,[1,2] NIANQIANG LI,[1,3] AND SHILONG PAN[2,*]

[1]School of Optoelectronic Science and Engineering, Soochow University, Suzhou 215006, China
[2]Key Laboratory of Radar Imaging and Microwave Photonics, Ministry of Education, Nanjing University of Aeronautics and Astronautics, Nanjing 210016, China
[3]e-mail: nli@suda.edu.cn
*Corresponding author: pans@nuaa.edu.cn

Received 8 August 2019; revised 29 August 2019; accepted 30 August 2019; posted 3 September 2019 (Doc. ID 375037); published 30 September 2019

Photonic microwave harmonic down-conversion is demonstrated using an optically injected semiconductor laser operating at period-one (P1) nonlinear dynamics. In this method, the P1 oscillation is stabilized through low-frequency local oscillator signal modulation, thus generating high-order harmonics in the optical domain. Meanwhile, a radio-frequency (RF) signal is received by an intensity modulator. After the subsequent optical heterodyning, photonic microwave harmonic down-conversion can be realized. In the proof-of-concept experiment, the 4th, 6th, 9th, and 12th harmonic down-conversions are demonstrated; i.e., an RF signal with a frequency of 39 GHz is down-converted to frequency-tunable intermediate frequency (IF) signals within 2 GHz. The resultant IF signal mainly holds the microwave linewidth and phase noise comparable to those of the original high-frequency one.

https://doi.org/10.1364/OL.44.004869

A microwave down-converter (MDC) is an essential module in various microwave systems such as wireless communication, radar, and electrical warfare [1]. Its functionality is to translate a received radio-frequency (RF) signal to a lower intermediate frequency (IF) signal with the help of a local oscillator (LO) signal. Traditional MDCs are based on pure electrical techniques, and thus suffer from narrow bandwidth, limited frequency, low isolation, and severe electromagnetic interference. Such MDCs cannot meet the requirements of many modern applications, which have been moving toward the millimeter-wave region. Fortunately, a few photonic microwave down-conversion approaches, with a higher frequency, wider bandwidth, a higher isolation, and immunity to electromagnetic interference, have been proposed [2–9]. Most of the photonic MDCs are realized by cascaded or paralleled electro-optic modulation and the subsequent photodetection [3–5]. In these schemes, RF and LO signals are applied to the two separate modulators, e.g., two Mach–Zehnder modulators (MZMs) [3,4] or two phase modulators (PMs) [5]. In order to down-convert a high-frequency RF signal, a high-performance LO signal in the same frequency band is required, which inevitably increases the overall cost and complexity. To cope with this, photonic microwave harmonic down-conversion methods have been proposed [6–9]. They can essentially lower the demand for the LO frequency, and thus only a fraction of the original frequency is needed. In [6] and [7], harmonic frequency down-conversion based on a mode-locked laser is verified. However, the repetition rate of the passively mode-locked laser is usually fixed, therefore limiting the frequency tunability of the down-converter. In [8] and [9], a optical frequency comb (OFC) is introduced to perform the frequency harmonic down-conversion, superior in the frequency tunability of the IF signal by simply adjusting the LO frequency. The main drawback of the OFC-based harmonic down-converter lies in its complex structure, i.e., consisting of multiple electro-optic modulators or semiconductor optical amplifiers, as well as requiring precise phase and/or amplitude control of the electrical driving signal.

In this Letter, we propose and experimentally demonstrate a photonic microwave harmonic down-conversion approach using an optically injected semiconductor laser (SL) operating at period-one (P1) nonlinear dynamics. To stabilize the P1 oscillation, a low-frequency LO signal modulation is adopted, which yields high-order harmonics in the optical domain. Meanwhile, the RF signal is received by an intensity modulator. Specifically, photonic microwave down-conversion of the 4th, 6th, 9th, and 12th harmonics can be demonstrated after the subsequent optical heterodyning. Thanks to the flexible and rich high-order harmonics, the proposed down-converter has the advantages of high operation frequencies and wide tunability. For example, an RF signal with a frequency as high as 39 GHz is down-converted to various IF signals within 2 GHz by the locked P1 dynamics. The microwave linewidth and phase noise performance of the resulting IF signals are also analyzed and satisfactory when compared to those of the input RF signal. To the best of our knowledge, this is the first photonic microwave harmonic down-converter (MHDC) based on an optically injected SL, which might greatly reduce the system cost and complexity.

The schematic diagram of the proposed photonic MHDC is presented in Fig. 1(a). A continuous wave (CW) light with a frequency f_m from a tunable laser source (TLS) is split into two parts. In the upper branch, the CW light is modulated by an RF signal with a frequency f_{RF} in an MZM. At the output of the MZM, an optical double-sideband (DSB) signal can be obtained. In the lower branch, the CW light is injected to a SL through an optical circulator. A polarization controller (PC) is used to align the polarization of the injection light with that of the SL to maximize the injection efficiency. Under the proper injection power and detuning frequency, the P1 oscillation states can be excited through undamping the relaxation resonance [10,11]. The output intensity of the SL shows self-sustained intensity oscillation with a frequency f_o. Its optical spectrum exhibits highly asymmetric DSB features. By simply varying the injection strength and/or the detuning frequency, the P1 frequency f_o can be tuned from a few to over 100 GHz [12]. In this Letter, the injection strength is defined as the square root of the power ratio between the injected light and the free-running SL. In our scheme, the P1 frequency f_o is tuned to slightly smaller than the RF frequency f_{RF} to obtain a low-frequency IF signal. Owing to the laser intrinsic noise, the microwave stability of the P1 oscillation is poor, however. As a result, the generated microwave signal has a broad linewidth and severe frequency jitter [13–15]. To utilize the P1 dynamics for photonic microwave down-conversion, both the poor spectral purity and the frequency stability need to be improved. In order to stabilize the P1 oscillation, an external subharmonic microwave modulation technique is adopted here [16,17]. An LO signal with a frequency $f_{LO} \approx f_o/n$ (n is a positive integer) is applied to modulate the SL. As shown in Fig. 1(b), with a proper modulation power, the modulation sidebands around the injection light at $f_m \pm nf_{LO}$ and P1 oscillation sidebands at $f_m \pm f_o$ become mutually locked. Consequently, the P1 oscillation is stabilized, while the P1 frequency f_o is locked and driven to nf_{LO}. Afterward, the optical signals in the two branches are combined, and optical spectrum at point B is illustrated in Fig. 1(c). As can be seen, the down-converted IF signal at $f_{IF} = f_{RF} - nf_{LO}$ can be generated by beating the RF-modulated sidebands and the stabilized P1 oscillation sidebands. After implementing the subsequent photodetection and low-pass filtering processing, the nth harmonic down-converted IF signal is generated.

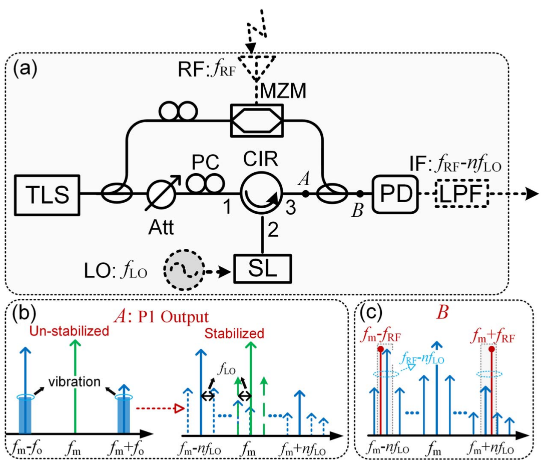

Fig. 1. (a) Schematic of the proposed photonic microwave harmonic down-converter. (b), (c) Optical spectra at point A and point B. TLS, tunable laser source; Att, optical attenuator; PC, polarization controller; CIR, optical circulator; SL, semiconductor laser; MZM, Mach–Zehnder modulator; PD, photodetector; LPF, low-pass filter.

It should be pointed out that our approach allows for P1 oscillation in the frequency range as large as 100 GHz and for the subharmonic modulation frequency (i.e., f_{LO}) as low as $1/n$ of P1 frequency. This indicates that our photonic MHDC has the advantages of a wide frequency range, flexible harmonic factors, and a low LO frequency. Additionally, the obtained IF frequency can be finely tuned by simply adjusting the LO frequency.

An experiment is carried out to verify the feasibility of the proposed method based on the setup in Fig. 1(a). The SL is a commercial distributed feedback laser (Actech LD15DM) biased at 30 mA, sufficiently above the threshold. Its free-running frequency and power are 194.223 THz and 4.24 dBm, respectively. The frequency of the TLS (Agilent N7714A) is set to be 194.249 THz, corresponding to a master-slave detuning frequency of 26 GHz. An RF signal generated by a microwave signal generator (Agilent E8257D) is received at a 40-GHz MZM (Fujitsu FTM7938EZ). The electrical LO signal is generated by another microwave signal generator (Agilent N5183B). A 40-GHz PD (u2t PDV2120RA) and a 2.3-GHz LPF are employed to attain the output IF signal. Electrical spectral properties are measured by an electrical spectral analyzer (ESA, R&S FSV40), and the optical spectrum is monitored by an optical spectrum analyzer (OSA, Yokogawa AQ6370C).

First of all, the electrical LO signal is not applied. The free-running P1 oscillation frequency f_o equals to 37.0 GHz, when the injection strength is adjusted to 1.58. The optical spectrum of the P1 dynamics is measured at port 3 of the optical circulator (point A), and the corresponding result is shown in Fig. 2(a) (blue curve). For comparison, the optical spectra of the injection light (black curve) and the free-running SL (red curve) are also displayed in Fig. 2(a). It can be clearly seen that there exist two highly dominant wavelength components separated by a P1 oscillation frequency of 37.0 GHz due to optical injection. The electrical spectrum of the generated 37.0-GHz signal is presented in Fig. 2(b), where the inset shows details in the span of 100 MHz. One can observe that the directly generated P1 oscillation signal has poor spectral

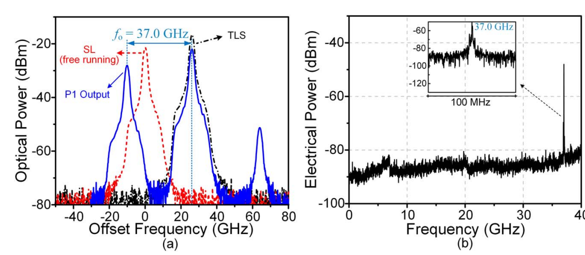

Fig. 2. (a) Optical spectra of the injection light (black), the free-running SL (red), and the injected SL (blue) when injection strength equals to 1.58. The x axis is relative to the free-running frequency of the SL. (b) Electrical spectrum of the generated P1 signal, resolution bandwidth (RBW) = 3 MHz. Inset: zoom-in view of the un-stabilized P1 signal (Span = 100 MHz, RBW = 200 kHz).

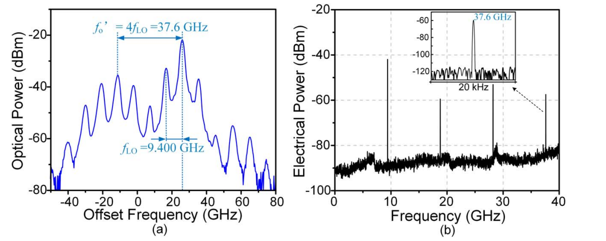

Fig. 3. (a) Optical and (b) electrical spectrum of the stabilized P1 oscillation with 1/4 subharmonic microwave modulation, RBW = 3 MHz. Inset: zoom-in view of the stabilized P1 signal (Span = 20 kHz, RBW = 200 Hz).

purity and a high noise floor, hardly meeting the requirement of photonic microwave down-conversion.

In order to stabilize the P1 oscillation, an electrical LO signal with a frequency f_{LO} of 9.400 GHz and a power of 18 dBm is applied to modulate the SL. Figure 3(a) illustrates the resultant optical spectrum of the injected SL. As can be observed in Fig. 3(a), when the 1/4 subharmonic microwave modulation is adopted, the P1 oscillation frequency becomes 37.6 GHz, equal to 4 f_{LO}. Meanwhile, the sidebands of direct modulation with frequency f_{LO} also exist. Thanks to the 1/4 subharmonic microwave modulation, the generated microwave signal is stably locked with a much smaller linewidth. It is interesting to find that the 3-dB linewidth of the 37.6-GHz signal is reduced to 200 Hz (equals to the RBW value), as shown in the inset of Fig. 3(b). Compared to the results in Fig. 2(b), i.e., the case of the free-running P1 oscillation signal, the spectral purity and the signal-to-noise ratio (SNR) of the stabilized P1 oscillation signal have been greatly improved.

In the upper branch, an RF signal with a frequency f_{RF} of 39 GHz is received at the MZM to obtain an optical DSB signal. Afterward, optical signals in the two branches are combined in an optical combiner, and the optical spectrum at point B is displayed in Fig. 4(a). In the optical spectrum, the marked area includes the RF-modulated sidebands as well as the stabilized P1 oscillation sidebands, and their frequency differences to the injection light are f_{RF} and $4f_{LO}$, respectively. After following photodetection and low-pass filtering, the 4th harmonic down-converted IF signal is produced. Figure 4(b) presents the electrical spectrum, exhibiting an IF frequency of $f_{IF} = f_{RF} - 4f_{LO} = 1.4$ GHz. The inset in Fig. 4(b) shows the detailed spectrum of the 1.4-GHz signal whose 3-dB linewidth is measured to be 200 Hz.

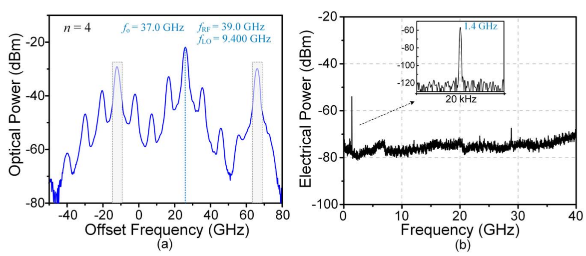

Fig. 4. (a) Optical spectrum before photodetection (point B). (b) Electrical spectrum of the 1.4-GHz IF signal, RBW = 3 MHz. Inset: zoom-in view of the IF signal (Span = 20 kHz, RBW = 200 Hz).

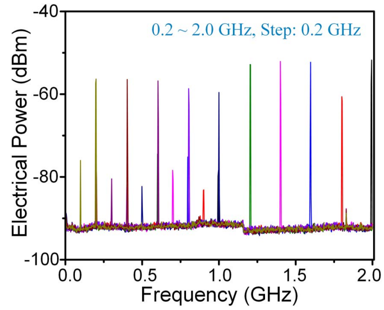

Fig. 5. Measured electrical spectra of the down-converted IF signals at different frequencies from the same 39-GHz RF signal (Span = 2 GHz, RBW = 1 MHz).

The tunability of the proposed system is also investigated. In the experiment, the 39-GHz RF signal can be down-converted to IF signals within 2 GHz by the locked P1 dynamics. As shown in Fig. 5, the IF signals from 0.2 GHz to 2.0 GHz are generated with a step of 0.2 GHz by tuning the LO frequency from 9.25 GHz to 9.70 GHz with a step of 0.05 GHz. Such property enables flexible harmonic down-conversion in a broad range of applications. For example, in an instantaneous frequency measurement receiver, the RF frequency can be measured by calculating the sum of the IF frequency and the 4th harmonic of the LO frequency, i.e., $f_{RF} = f_{IF} + 4f_{LO}$.

The harmonic factor of the proposed photonic MHDC can be further changed. The feasibility of the 6th, 9th, and 12th harmonic down-conversions is also demonstrated. The optical spectra before photodetection and electrical spectra of the generated IF signals for high-order harmonic down-conversion are evaluated, with the results shown in Figs. 6(a) and 6(b),

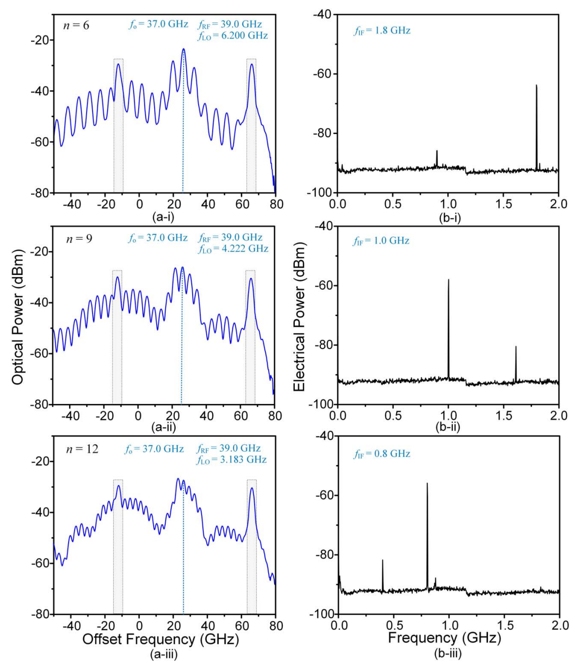

Fig. 6. (a-α) Optical spectra before photodetection (point B). (b-α) Electrical spectra of the IF signals, RBW = 1 MHz. α equals to i, ii, and iii, for the harmonic factor n of 6, 9, and 12, respectively.

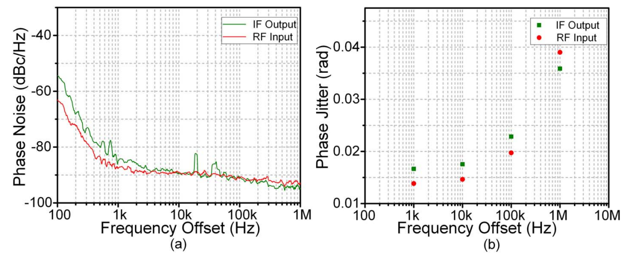

Fig. 7. Comparison of the (a) phase noise spectra, (b) integrated phase jitter between the input RF signal and the output IF signal, when the harmonic factor n equals to 12.

respectively. In Figs. 6(a-i) and 6(b-i), the 39-GHz RF signal has been down-converted to a 1.8-GHz IF signal through the 6th harmonic down-conversion by a 6.200-GHz LO signal. Likewise, Figs. 6(a-ii) and 6(b-ii) correspond to the case of the 9th harmonic by a 4.222-GHz LO signal, resulting in a 1.0-GHz IF signal; and Figs. 6(a-iii) and 6(b-iii) represent the case of the 12th harmonic by a 3.183-GHz LO signal, leading to a 0.8-GHz IF signal. It is worth noting that harmonic down-conversion is also proved for other harmonic factors n within 12. These results confirm that the proposed harmonic down-conversion approach is effective for a harmonic factor up to 12.

Finally, the phase noise performance is analyzed, where the SSB phase spectra for both before and after harmonic down-conversion are measured. As an example, Fig. 7(a) provides a comparison of the phase noise spectra between the input RF signal and the output IF signal, with harmonic factor n being 12. Compared with the 39-GHz RF signal, the 0.8-GHz IF signal has a similar phase noise performance at offset frequencies above 10 kHz, although its phase noise at lower offset frequencies is slightly higher. For comparison, the integrated phase jitter is also calculated. Figure 7(b) illustrates the phase jitter integrated from 100 Hz to the considered frequency. Again, the IF signal has a slightly higher phase jitter at lower offset frequencies, which coincides with Fig. 7(a). We note that the phase noise of the IF signal is not only affected by the acoustic noise from the optical heterodyne structure, but also by the performance of the stabilized P1 signal. Various active/passive methods could be employed to overcome the former noise, e.g., [18,19]. As for the realization of a high-purity P1 oscillation, the modulation parameters, i.e., the power and the frequency of the LO signal, should be set within a rigorous range for proper locking. This property has been thoroughly studied in the prior work [16] and is not the focus of the current contribution.

In conclusion, we have proposed and experimentally demonstrated a photonic MHDC based on stabilized P1 nonlinear dynamics of SLs. In this method, the P1 oscillation is stabilized through $1/n$ subharmonic modulation using a low-frequency LO signal. Then, harmonic down-conversion is achieved by beating the stabilized P1 oscillation sidebands and the RF-modulated sidebands. In the experiment, the 4th, 6th, 9th, and 12th harmonic down-conversions are demonstrated. An RF signal with a frequency as high as 39 GHz is down-converted to IF signals within 2 GHz through the locked P1 dynamics. In addition, the microwave linewidth and phase noise are well preserved after harmonic down-conversion. The proposed photonic MHDC features a wide frequency range, flexible harmonic factors, a low LO-frequency, and a simple structure.

Furthermore, it has been recognized that the direct modulation bandwidth of a SL can be significantly enhanced over 3 times the intrinsic bandwidth by optical injection locking [20]. Therefore, the MZM can be replaced by another SL in the upper branch of the proposed scheme, leading to a modulator-free photonic MHDC, which can further reduce the cost and size.

Funding. National Key Research and Development Program of China (2018YFB2201803); Startup Funding for Outstanding Young Scholars of Soochow University (GJ15900519).

REFERENCES

1. X. Ye, F. Zhang, Y. Yang, and S. Pan, Photon. Res. **7**, 265 (2019).
2. J. Yao, J. Lightwave Technol. **27**, 314 (2009).
3. G. Gopalakrishnan, R. Moeller, M. Howerton, W. Burns, K. Williams, and R. Esman, IEEE Trans. Microwave Theory Tech. **43**, 2318 (1995).
4. E. H. W. Chan and R. A. Minasian, J. Lightwave Technol. **30**, 3580 (2012).
5. V. R. Pagán, B. M. Haas, and T. E. Murphy, Opt. Express **19**, 883 (2011).
6. P. Ghelfi, G. Serafino, F. Scotti, F. Laghezza, and A. Bogoni, Opt. Lett. **37**, 3924 (2012).
7. J. Liao, X. Zheng, S. Li, H. Zhang, and B. Zhou, Opt. Lett. **39**, 6565 (2014).
8. Y. Zhao, X. Pang, L. Deng, X. Yu, X. Zheng, and I. T. Monroy, IEEE Photon. Technol. Lett. **24**, 16 (2012).
9. X. Zou, S. Zhang, H. Wang, Z. Zhang, J. Li, Y. Zhang, S. Liu, and Y. Liu, IEEE Photon. J. **10**, 5500308 (2018).
10. T. B. Simpson, J. M. Liu, K. F. Huang, and K. Tai, Quantum Semiclass. Opt. **9**, 765 (1997).
11. S. K. Hwang, J. M. Liu, and J. K. White, IEEE J. Sel. Top. Quantum Electron. **10**, 974 (2004).
12. P. Zhou, F. Zhang, Q. Guo, S. Li, and S. Pan, IEEE J. Sel. Top. Quantum Electron. **23**, 1 (2017).
13. J. P. Zhuang and S. C. Chan, Opt. Express **23**, 2777 (2015).
14. S. Ji, C. Xue, A. Valle, P. S. Spencer, H. Li, and Y. Hong, J. Lightwave Technol. **36**, 4347 (2018).
15. M. J. Wishon, D. Choi, T. Niebur, N. Webster, Y. K. Chembo, E. A. Viktorov, D. S. Citrin, and J. K. White, IEEE Photon. Technol. Lett. **30**, 1597 (2018).
16. L. Fan, Z. M. Wu, T. Deng, J. G. Wu, X. Tang, J. J. Chen, S. Mao, and G. Q. Xia, J. Lightwave Technol. **32**, 4058 (2014).
17. P. Zhou, F. Zhang, D. Zhang, and S. Pan, Opt. Lett. **43**, 5439 (2018).
18. M. Kaba, H.-W. Li, A. S. Daryoush, J.-P. Vilcot, D. Decoster, J. Hazelas, G. Bouwmans, Y. Quiquempois, and F. Deborgies, IEEE Microw. Mag. **7**(4), 38 (2006).
19. Y. Zhang, D. Hou, and J. Zhao, J. Lightwave Technol. **32**, 2408 (2014).
20. S. K. Hwang, J. M. Liu, and J. K. White, IEEE Photon. Technol. Lett. **16**, 972 (2004).